Tunnelling and Underground Space Technology 71 (2018) 27–35

Contents lists available at ScienceDirect

Tunnelling and Underground Space Technology

journal homepage: www.elsevier.com/locate/tust

An in-tunnel grouting protection method for excavating twin tunnels beneath an existing tunnel

Dalong Jin*, Dajun Yuan, Xinggao Li, Haotian Zheng

Key Laboratory of Urban Underground Engineering of the Education Ministry, Beijing Jiaotong University, Beijing 100044, China

ARTICLE INFO

Keywords:
Twin tunnels
Settlement and stress
Under-crossing
Tunnel behavior

ABSTRACT

A section of closely spaced twin tunnels at Shangmeilin station on Shenzhen metro line 9 was excavated by the shield tunneling method. Part of this section lies closely beneath the tunnel servicing Metro line 4. Due to restrictions on ground surface to control the extra settlement of the existing tunnel in the area, an in-tunnel grouting protection method was adopted in combination with the shield method. This method greatly reduced the effect on the existing tunnels when building the twin tunnels underneath. The settlement of and stress on the existing tunnels associated with the construction of the new tunnels were systematically monitored. Because of the twice under-crossing process, the excavation of twin tunnels had a superposed influence on the existing tunnel and surrounding soil. The behavior of the overlying tunnel was analyzed based on instrumentation records obtained from the project. The settlement profile of the existing structure displayed a "V" shape after the first under-crossing but a "W" shape after the second. The hoop stress of the existing tunnel induced by shield tunneling below had beneficial effects on the stress state of the tunnel structure. By contrast, the longitudinal stress exerts a bending moment on the existing tunnel, with a large tensile stress that had adverse effects on its structure. Based on the monitored data, three deformation modes are proposed to describe the behavior of the existing tunnel. In addition, the differences between the two under-crossing processes are discussed; both the ground loss ratio and width parameter of the settlement trough in the second profile were larger than those of the first profile due to the decrease in soil stability.

1. Introduction

When tunneling in densely populated urban areas, new tunnels are inevitably constructed in close proximity to existing underground structures. In these cases, an earth pressure balanced (EPB) shield machine is widely used. During the mechanized tunneling process, the influence of shield tunneling on the surrounding soil or existing structures is not negligible and is closely related to the soil properties, working parameters of the shield machine, and the depth of the overburden soil. In particular, building twin closely spaced tunnels under an existing tunnel can lead to greater tunnel deformation and ground settlement due to the dual disturbances caused by tunnel excavation. In these cases, it is highly difficult to control the deformation of the existing tunnel, which might not only lead to excessive deformations of the existing nearby tunnel but also pose a serious threat to tunnel operation safety. Protective measures must be considered and analyzed in the design phase to ensure safe construction as well as the operation of the existing tunnel.

The construction of a tunnel, which depends greatly on the ground condition, must be carefully designed in terms of risks and uncertainties to ensure the final objective of quality (e.g., Oggeri and Ova, 2004; Wood, 2002). A substantial number of studies have investigated ground movements as well as the deformation of existing tunnels induced by the construction of a new tunnel (e.g., Attewell and Woodman, 1982; Cooper et al., 2002; Fang et al., 2015; Li and Yuan, 2012; Peck, 1969; Schmidt, 1969; Yamaguchi et al., 1998). The implementation of appropriate supplementary countermeasures to reduce the deformation of ground or subsurface structures nearby is crucial. Grout technology is widely used to condition the soil and protect existing structures in EPB shield tunneling. Garshol (2003) indicated that pre-excavation grouting or pre-grouting is conducive to the improvement of ground stability and ground water control in rock. The operational process, supporting devices and main technical characteristics of grouting were presented. Kovári and Ramoni (2004) summarized the construction experiences of urban tunneling in soft ground and concluded that the design procedure demands high reliability, including statistical calculations for the determination of the necessary support pressure or shape, size and quality of the grouted body. Li et al. (2013) presented a case of an in-tunnel

* Corresponding author.
E-mail address: jindalong@163.com (D. Jin).

http://dx.doi.org/10.1016/j.tust.2017.08.002
Received 22 May 2016; Received in revised form 21 January 2017; Accepted 1 August 2017
0886-7798/

jacking above the tunnel protection methodology for excavating a tunnel under a tunnel in service. Kimpritis (2014) explained how jet-grouting can be used as an integral part of complex tunneling projects and summarized the basic framework for the design and execution of jet-grouting in tunneling. Ye et al. (2015) analyzed the mechanism of an unexpected ground surface settlement of approximately 0.8 m in a Double-O-Tube (DOT) tunnel construction site in Shanghai; the ground settlement was reduced to approximately 0.02 m after implementing improved grouting measures.

According to the literature, there is very limited knowledge on the influence of shield tunneling on overlying existing tunnels and the measures used to reduce the overlying tunnel deformation induced by excavation of new twin tunnels below. Most conventional countermeasures cannot be directly adopted because of the confined space, limited headroom, and the required level of safety and efficiency. This paper describes the implementation of an effective protection method of grouting in existing tunnels for excavating under-passing twin tunnels to control the settlement of an overlying tunnel in China metro construction. This method controls the tunnel deformation and thus decreases the additional stress placed on the existing tunnel. The method aims to compensate for the ground loss induced by tunneling below and reinforce the surrounding soil before construction of new twin tunnels. The displacement of the existing tunnel was controlled within an allowable value using this method. In addition, both the cross-sectional and longitudinal changes in the existing tunnel, including deformation and stress as well as the interaction of the twin tunnels, are investigated in this paper. The deformation characteristics of the existing tunnel in the first and second under-passing are compared based on the monitoring data.

2. Project overview

The plan view and cross-sectional view of the existing and new tunnels at the Shangmeilin station in Shenzhen are shown in Figs. 1 and 2, respectively. The existing tunnels in service run east–west and belong to line 4 of the Shenzhen metro. The tunnels are horizontally parallel and were excavated by the shield method four years ago. The distance between the right tunnel and left tunnel is 7.2 m. The outer and the inner radii of the precast segmental lining are 3.0 m and 2.7 m, respectively. The width of each segment is 1.5 m. The depth of the existing tunnels is approximately 12 m.

The new shield twin tunnels were completed in 2015 as part of the Shenzhen metro line 9. The clearance between the right tunnel and left tunnel is 8.0 m. The clear distances from the new tunnels to the existing tunnels is approximately 2.5 m, and there is a skew of 83 °between the new tunnels and the existing tunnels. The thickness of the segment is 300 mm, and the width is 1.5 m. The segmental lining consists of five segments with a key segment (Fig. 3). The ground surface is at the intersection of two crowded roads, Meilin Road and Zhongkang Road. The first under-crossing of the right tunnel of Line 9 began on the night of 14 November and ended on the afternoon of 18 November. The second under-crossing of the left tunnel began approximately one month later, on the night of 12 December, and ended on the night of 16 December. One Herrenknecht AG shield machine and one Wirth shield machine with excavation diameters of 6280 mm and lengths of approximately 7.9 m and 13.0 m, respectively, were used to build the new tunnels. Before driving, the shield machines were thoroughly inspected and maintained, and all cutting tools were replaced to avoid breakdown of the shield machine below the existing tunnel.

As shown in Fig. 2, the subsurface ground at the site is very complex and consists of back fill, silt clay, sandy soil, gravelly soil and completely weathered granite. The mean values of the physical and mechanical parameters of the soils retrieved from the site investigation report are shown in Table 1.

3. Protection schemes in the design phase

The existing tunnel is just below a busy street, as shown in Fig. 1. It was difficult to adopt reinforcement measures to ensure the safety of the existing tunnel when constructing the twin tunnels. In this case, an in-tunnel grouting protection method was adopted to control the deformation of the existing tunnels. This scheme aimed to compensate for the ground losses caused by the excavation of the new tunnel below. As shown in Fig. 4, grouting pipes with a length of 2.0 m were symmetrically installed in the grout holes in the lining segment of the existing tunnel at an interval of 3.0 m. As the excavation of the new twin tunnels of line 9 would cause twice as many disturbances of the surrounding soil, the corresponding angles of influences, as shown in Fig. 3, may be generally expressed as $\beta = 45° + \varphi/2$, where φ denotes the intrinsic soil friction angle (see Fig. 5).

A two-component grout method was adopted in this study. This grout method was developed to achieve good workability and quick

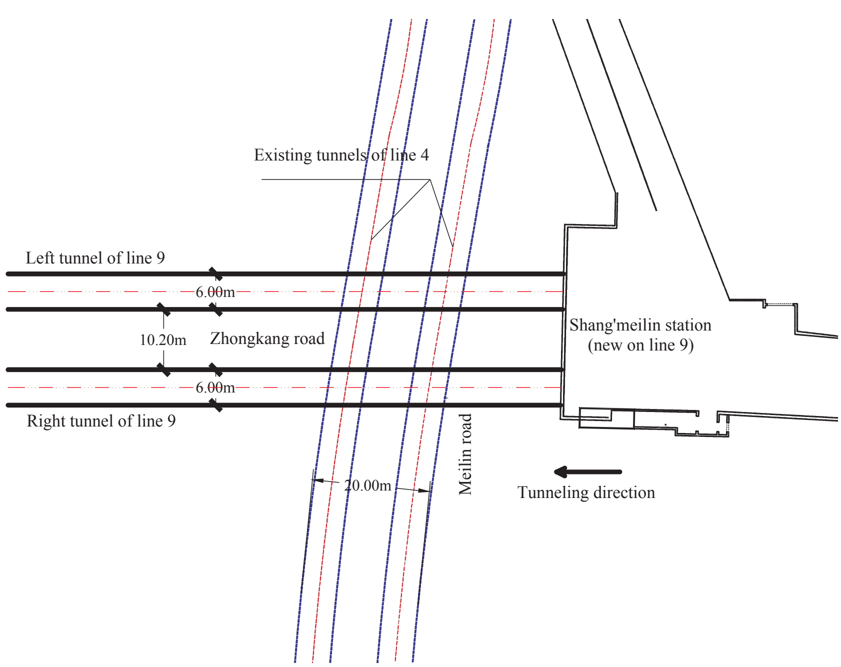

Fig. 1. Plan view of the existing tunnels and the new twin tunnels.

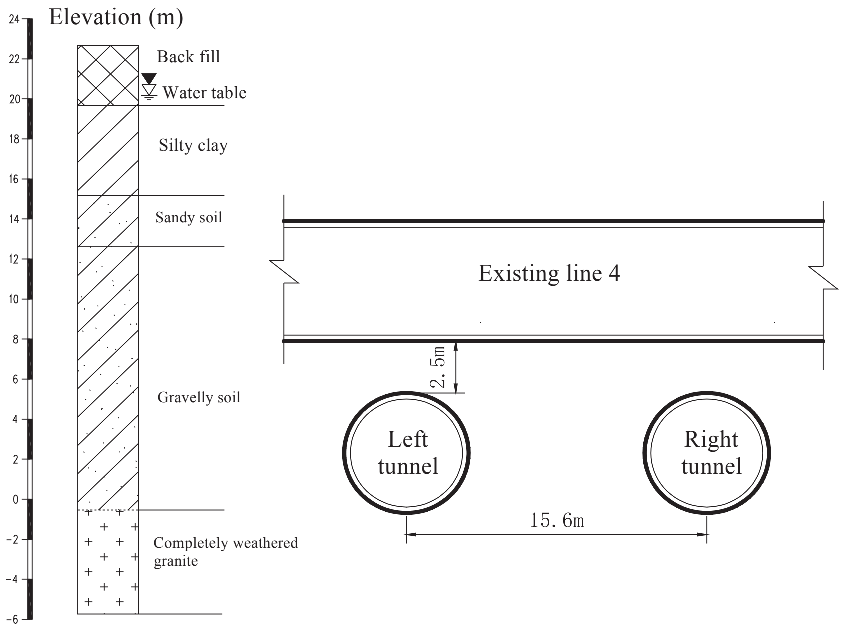

Fig. 2. A typical cross-section showing the existing tunnels, the new twin tunnels, and the soil profile.

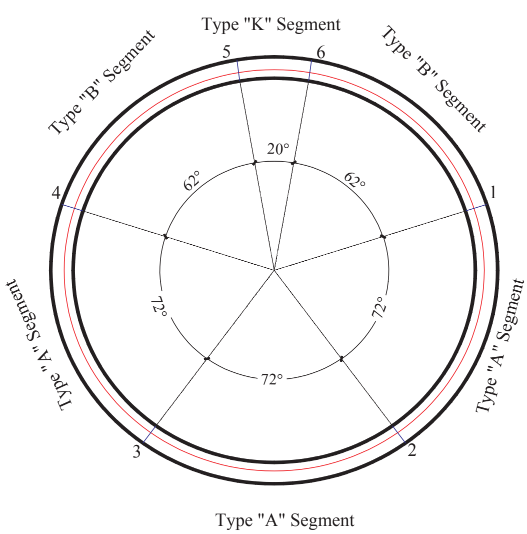

Fig. 3. Cross-section of the existing precast segmental lining.

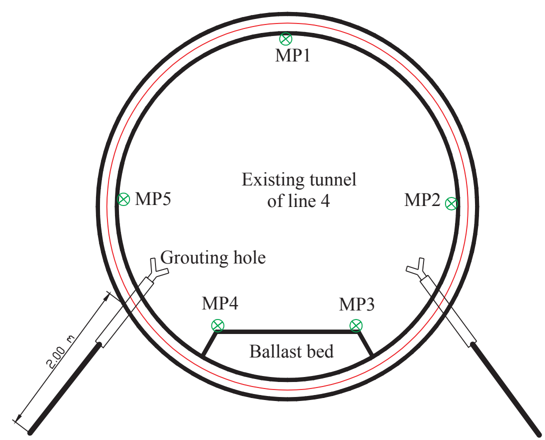

Fig. 4. The position of the grouting holes in the existing tunnel and the layout of the deformation measuring points.

setting. Both components had a slurry consistency that enabled them to be pumped close to the grout holes, where they were mixed. One component was a cement bentonite slurry, and the other component was water glass, which is a mixture of sodium silicate and water. After a short reaction time, a gel was formed. The grout reaction time can be adjusted by controlling the volume flow of the two components. The stiffening behavior of the two-component grout was similar to the stiffening behavior of hydraulic setting mortar. The initial setting time of the grout was approximately 10 min, and the final setting time was approximately 25 min. As shown in Fig. 6, a double-piston pump was used to convey the slurry, and the volume of delivered mortar was regulated by the pace of the piston. Each piston filled one grout supply line with a component. The grout mixtures used in the two-component grout method are shown in Table 2.

When grouting through grout pipes in the existing tunnel, the following principles were strictly imposed. (a) Before the excavation of new tunnels below the existing tunnel, grouting was performed to pre-reinforce the surrounding soil, which had poor stability due to the vibrations of running trains. (b) During the construction of the new

Table 1
Physical and mechanical parameters of the soils.

ID	Soil layer	γ (kg/m^3)	e_o	C_{cu} (kPa)	φ_{cu} (°)	w_n (%)	I_p (%)	I_l (%)	SPT-N
1–1	Back fill	1950	0.72	10.0	12.0	21.3	15.6	0.11	4.3
3–2	Silty clay	1940	0.69	19.9	15.6	23.2	17.62	0.12	6.2
6–1	Sandy soil	1860	0.81	23	20	28.0			10.0
6–2	Gravelly soil	1900	1.12	24.0	22.0	26.0	12.8	0.80	16.0
11–1	Completely weathered granite	1960	1.02	27.6	20.4	23.8	10.4	0.06	45.5

Note: γ = unit weight; e_o = void ratio; w_n = natural water content; I_p = liquid index; wp = plasticity index; C_{cu} = cohesion of consolidated undrained triaxial compression test; φ_{cu} = friction angle of consolidated undrained triaxial compression test; SPT-N = number of standard penetration test.

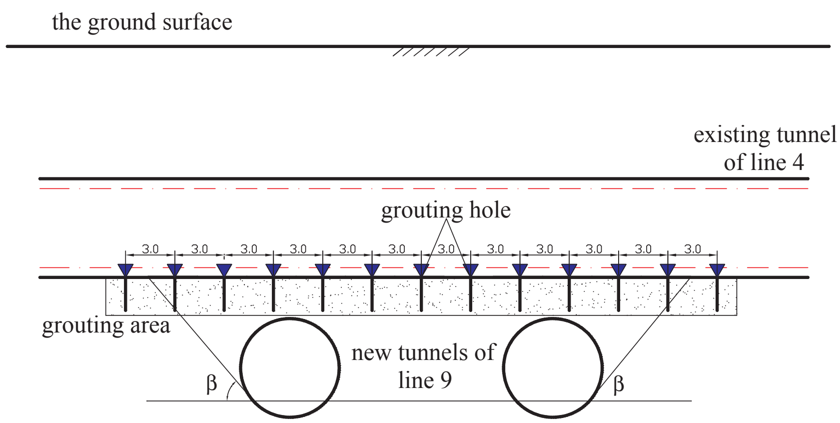

Fig. 5. The grouting holes along the existing tunnel.

Fig. 6. The double-piston pump.

Table 2
Proportions of the adopted two-component grout.

Two-component grout	Component A			Component B	
Mass	Cement (kg)	Bentonite (kg)	Water (kg)	Sodium silicate (kg)	Water (kg)
	248	20	124	98	294

tunnel beneath the existing tunnel, grouting was performed simultaneously to compensate for the loss of ground, rather than jacking up the existing tunnel using an external force. For this purpose, the required grouting pressure was less than 0.2 MPa, and the lower limit of grouting pressure was controlled based on the ability to inject grouting material. (c) This scheme emphasizes the deformation of the existing tunnel caused by under-crossing tunnels in different stages and stress monitoring. The measured data were processed in a timely manner and fedback to the related operators to realize an information-oriented project.

4. Monitoring and construction

4.1. Automatic monitoring system

The excavation of the new tunnel below has a large impact on the existing tunnel and can cause excess deformation or cracks in the structure. Monitoring the deformation of and additional stress on the existing tunnel induced by new shield tunneling is critical. The monitoring data reflects the impact on the tunnel structure and whether the structure is safe. During the new twin-tunnel construction, the deformation and additional stress of the existing tunnels, including both the hoop stress and longitudinal stress, were monitored. The layout of the monitoring points is shown in Fig. 7. Twenty-four monitoring cross sections along the surveyed length of 120 m in the existing tunnel were arranged to capture displacements of the existing tunnel. The parenthesized texts “MD” and “MS” in Fig. 7 denote the monitoring cross sections of tunnel deformation and additional stress, respectively. The spacing between the neighboring sections over the new shield tunnel was 3–4 m. The measuring point layout in each monitoring cross section is depicted in Figs. 8 and 9. The deformation monitoring points were monitored by an automatic total station system, which consisted of the automatic total station and reflecting prism. As shown in Fig. 10, the additional stress of the inner surface of the tunnel lining was monitored by strain gauges. Nine monitoring cross sections were arranged along the existing tunnel to obtain the additional stress to the tunnel induced by shield tunneling.

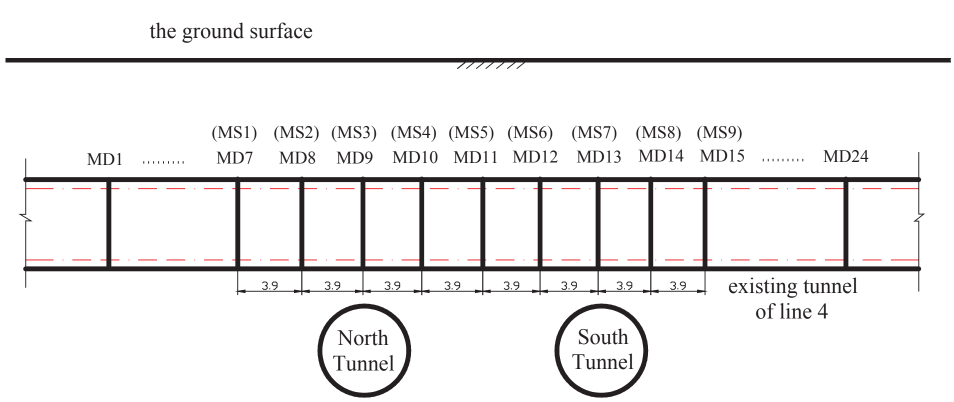

Fig. 7. Layout of the monitoring points along the existing tunnel sections.

Fig. 8. Measuring points of reflecting prisms.

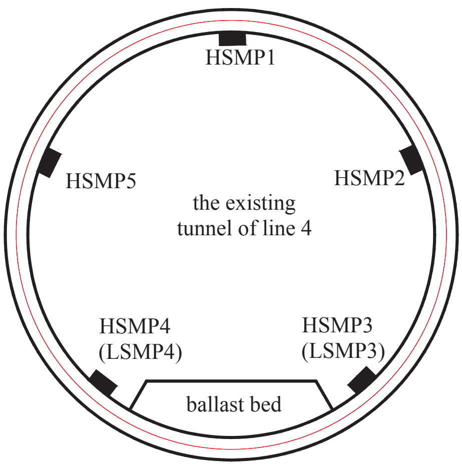

Fig. 9. Measuring points of strain gauges.

Fig. 10. Strain gauge installed in the segment.

4.2. Working parameters of the shield machine

The working parameters of the EPB shield machine can greatly affect adjacent structures, and the surrounding soil and must be controlled when tunneling below an existing tunnel. Good preparation and planning ensured that shield driving below the existing tunnel proceeded smoothly. During the first shield tunneling, the key parameters were as follows: the earth pressure in the excavation chamber approximately 0.2–0.3 MPa, the total thrust was approximately 1000–1100 t, the cutter head torque was approximately 1900–2100 kN·m, the cutter head rotation speed was approximately 1.4–1.6 rpm, the shield driving speed was approximately 40–50 mm/min, the muck discharged per ring was approximately 60–70 m^3, the simultaneous backfilling was approximately 6.0–7.0 m^3 per ring, and the injection pressure was approximately 3.0 bar. For the second undercrossing, the important shield tunneling parameters were adjusted to a total thrust of approximately 1100–1200 t, cutter head torque of approximately 1400–1700 kN·m, cutter head rotation of approximately 1.5–2.0 rpm, shield driving speed of approximately 40–45 mm/min, muck discharged per ring of approximately 60 m^3, simultaneous backfilling of approximately 6.0 m^3 per ring and an injection pressure of approximately 2.5–2.7 bar. The mix proportion of the adopted tail void grout is presented in Table 3. The foam injection ratio (FIR) was 20%, and the foam expansion ratio (FER) was 12. The concentration of foaming agent within the foaming liquid was 5.26%. The two shield machines worked exceptionally well in their under-crossings with minimum disturbances, resulting in only small settlements of the overlying tunnels.

Table 3
Mix proportion and performance parameters of the backfill grouting.

Compound	Cement	Bentonite	Fly ash	Sand	Water
Mix proportion (kg)	110	80	265	400	485
Initial setting time	150 min				
Strength-reaching time	6 h				

5. Characteristics of the behavior of the existing tunnels

5.1. Longitudinal responses of the existing tunnels

5.1.1. Settlement development of the existing tunnels

According to the monitoring data, the development of the settlements for the points immediately above the new tunnels are shown in Fig. 11. The ballast beds of the existing tunnel were greatly affected by shield excavation. The beds first underwent uplift and then subsidence, and the final settlements of the left tunnel and right tunnel were approximately 6.3 mm and 5.6 mm when the tunnels were in a relatively stable state.

The settlement of the existing tunnels experienced three stages. (a) The first stage was from line A to line B (A–B), where the shield cutter head had not reached the existing tunnel. In this stage, the shield thrust and friction between the shield machine and soil led to heaving of the existing tunnel of only 1.0 mm. (b) The second stage was from line B to line C (B–C). In this stage, the shield machine passed by the existing tunnel, and the interspaces of the shield tail were primarily responsible for the deformation of the soil mass and tunnel above due to shield tunnel construction. Therefore, the settlement of the existing tunnels increased rapidly and reached approximately 5.0–6.0 mm in this stage. Grouting in the existing tunnel reduced the displacement to control the settlement of the existing tunnel. (c) The third stage was from line C to line D (C–D). In this stage, the settlement curve became smooth as the shield machine moved away from the existing tunnel, and the deformation in this stage was primarily caused by soil consolidation.

5.1.2. Settlement profile of the existing tunnel

The first under-crossing began on November 14, 2015, and the second under-crossing began one month later. The settlement of the overlying tunnels after the first under-crossing and second under-crossing is shown in Fig. 12. The settlement of the existing tunnel induced by the first under-crossing shown in Fig. 12 was symmetric about the tunnel centerline. The maximum settlements of the left tunnel and right tunnel were approximately 6.0 mm and 5.0 mm, respectively. The longitudinal subsidence scope of the existing tunnel was approximately 50 m after the first under-crossing. The settlement profile of the existing structure displayed a “V” shape after the first under-crossing but a “W” shape after the second. The settlement of the existing tunnel after the

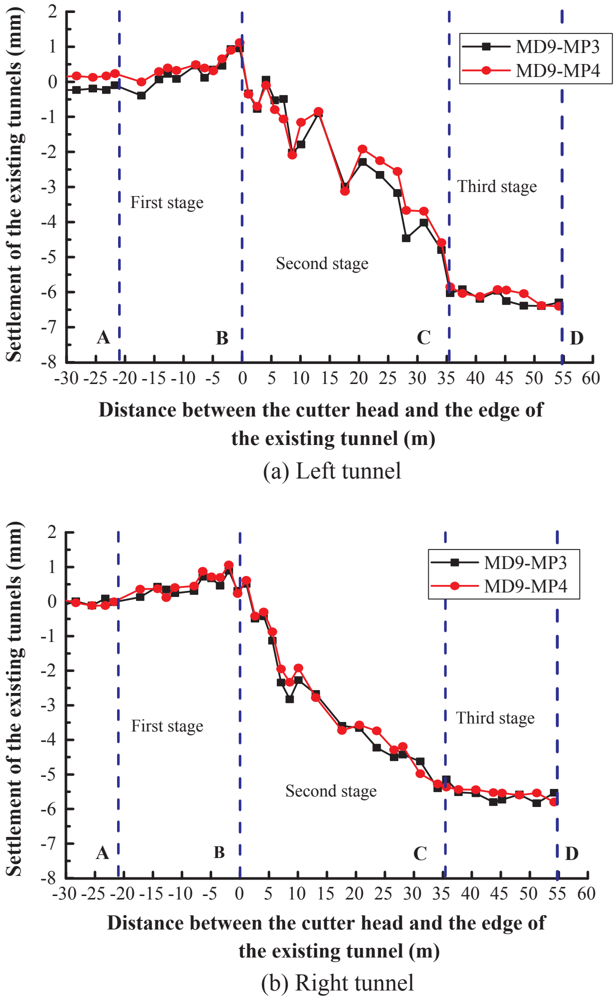

Fig. 11. Settlement development of the existing tunnels.

second under-crossing was apparently asymmetric. The longitudinal subsidence scope of the existing tunnel was larger than that of the first under-crossing, and the location of maximum settlement deviated from the original position. The maximum settlement increased by 50% to 8.3 mm (7.8 mm, the other tunnel) from 6.0 mm (5.0 mm, the other tunnel). These phenomena warrant closer attention in the construction of twin tunnels.

5.1.3. Longitudinal stress of the existing tunnels

The additional stress at the monitoring sections LSMP3 in MCS3, MCS4, MCS5 and MCS6 illustrate the response of the existing tunnel to the under-passing shield tunneling. As an example, the symbol "MCS3-LSMP4" represents monitoring point 4 of longitudinal stress at monitoring cross section 3. The additional stress induced by shield tunneling below is shown in Fig. 13. The additional stress at the related monitoring points revealed an increasing trend with time, and the bottom of the tunnel structure remained under tension. The additional stress at MCS5-LSMP3 and MCS6-LSMP3 was caused by both the first under-crossing and the second under-crossing, whereas the stress at MCS3-LSMP3 and MCS4-LSMP3 remained essentially stable in the second under-crossing and was not related to the shield tunneling below. The recorded maximum additional stress induced by shield tunneling below was approximately 0.7 MPa and occurred at MCS5-LSMP3. As the longitudinal differential settlement was relatively small before under-crossing, the recorded additional longitudinal stress of the existing tunnel in the process of under-crossing represents the real stress value. In this case, the existing tunnel can be damaged if the longitudinal

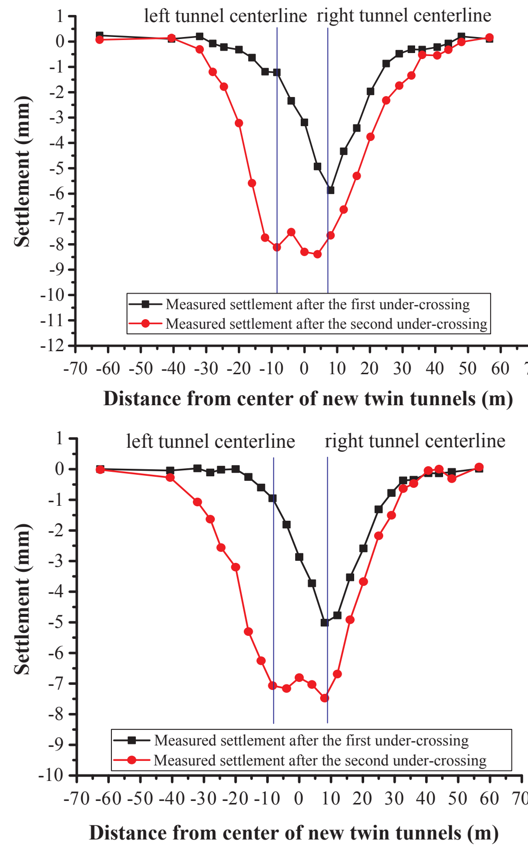

Fig. 12. Settlement profiles after two under-crossings.

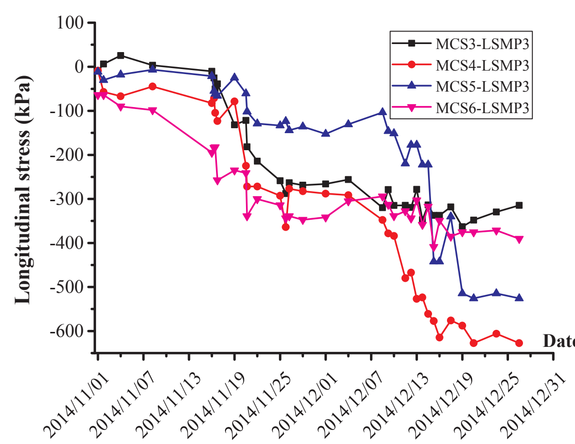

Fig. 13. The longitudinal stress of the existing tunnel.

stress is larger than the allowable value.

5.2. Response of the existing tunnel cross section

The characteristics of the influence of the excavation of a new tunnel on the cross-section of an existing tunnel are analyzed in this section. The sectional profiles of hoop stress and deformation induced by shield tunneling are shown in Fig. 14 and described below, and the relative measuring section is just above the new tunnel. Tensile stresses are considered negative and compressive stresses positive in Fig. 9. The various stages shown in the figure correspond to the construction phases outlined below (see Fig. 15).

Stage 1: The succeeding shield approached the measuring point, and

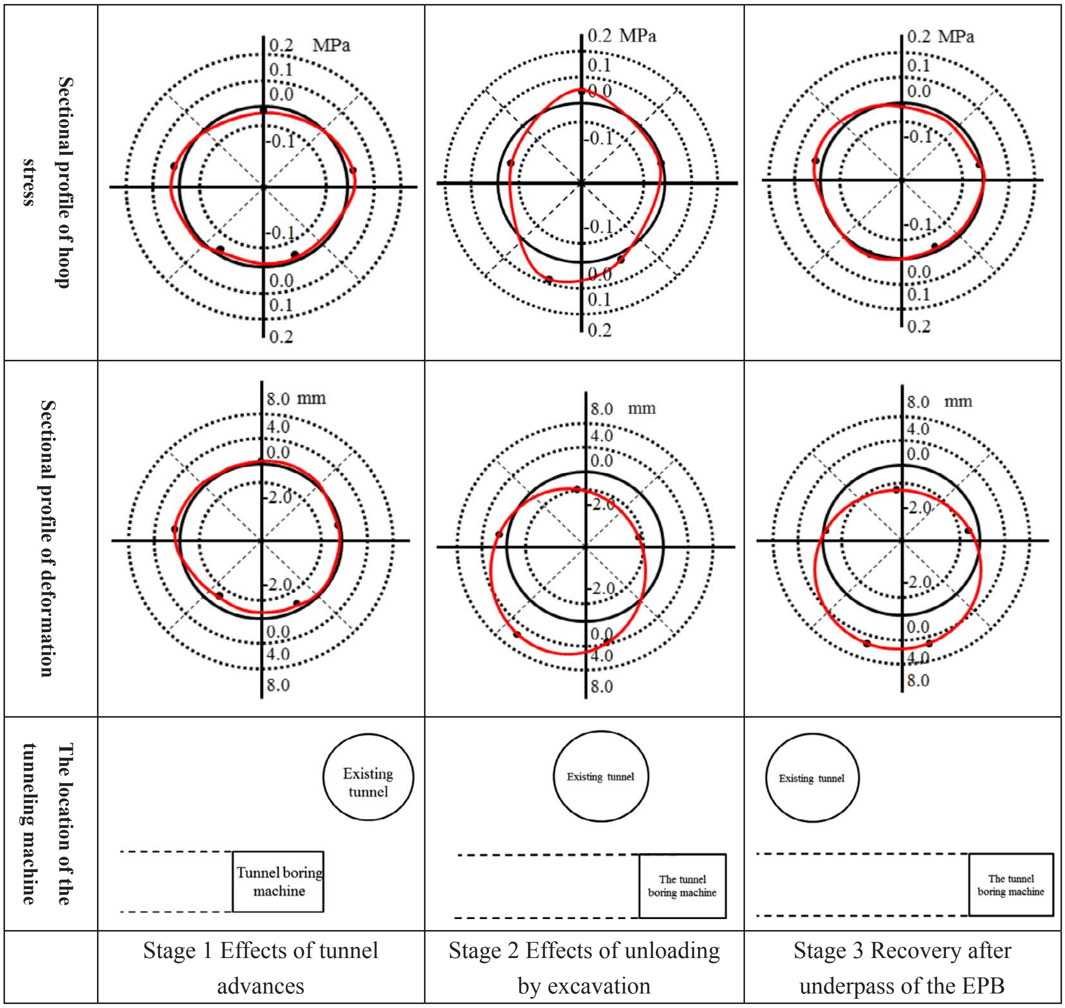

Fig. 14. Sectional profiles of hoop stress and deformation.

its thrust began to have an influence. Relative upheaval was observed at this section as the succeeding shield machine approached. The distorted shape of the preceding tunnel indicates that horizontal expansion occurred, and the vertical diameter decreased, while the horizontal diameter increased.

Stage 2: The tail of the succeeding shield machine passed the monitoring section, and the distorted shape of the preceding tunnel was a vertical expansion. There was an offset of the tunnel on the diagonal axis rather than principal axes. It is assumed that this deformation was a consequence of the reduced load on top of the tunnel caused by the excavation of the succeeding shield.

Stage 3: The shield machine moved far away and ceased to have any effect on the existing tunnel. The sectional force of the tunnel and the transition of the loads converged after the succeeding shield had passed. The distorted shape of the existing tunnel then returned to its original state. There was an offset of the tunnel section on the principal axes.

Fig. 14 shows three deformation modes of the existing tunnel section resulting from the new tunnel excavation. The influence of shield tunneling on the existing tunnel behavior was observed simultaneously as the load was imposed by the shield drive and the consequent unloading by excavation. These deformation modes were prompted by a combination of the influences from the driving thrust of the succeeding tunnel and the decrease of the load by excavation. High stress and non-uniform deformation occurred in the existing tunnel, and the overlying soil had a great effect on restricting ovalization of the tunnel. The maximum distortion occurred in stage 2 with a vertical expansion, and the maximum hoop stress was approximately 0.1 MPa. Importantly, the existing tunnel was built with a horizontal ovalization before the excavation of the new tunnel below. Therefore, hoop stress effects can be beneficial in the final condition.

6. Discussion

6.1. The key points of the construction process

The influence of shield tunneling on surrounding soil or existing structures is closely related to the soil properties, the earth pressure on the cutter face, the back-fill grouting and other working parameters of the EPB shield machine. These factors should be controlled carefully to ensure that the tunnel deformation satisfies the operating requirements. The key points of the shield tunneling process are listed below:

(a) Soil conditioning is very important to ensure adequate flow in the excavation chamber and the screw conveyor. Thus, soil conditioning facilitates stabilization of the tunnel face and is a useful strategy for reducing existing tunnel deformation.
(b) The reasonable support pressure must be determined by shield tunneling in the test section before the under-crossing process. Unbalanced earth pressure on the cutter face can cause serious deformation of the existing tunnel.
(c) The settlement of the existing tunnel increases rapidly after the tail passes, and the tail void is the dominant factor in the deformation of

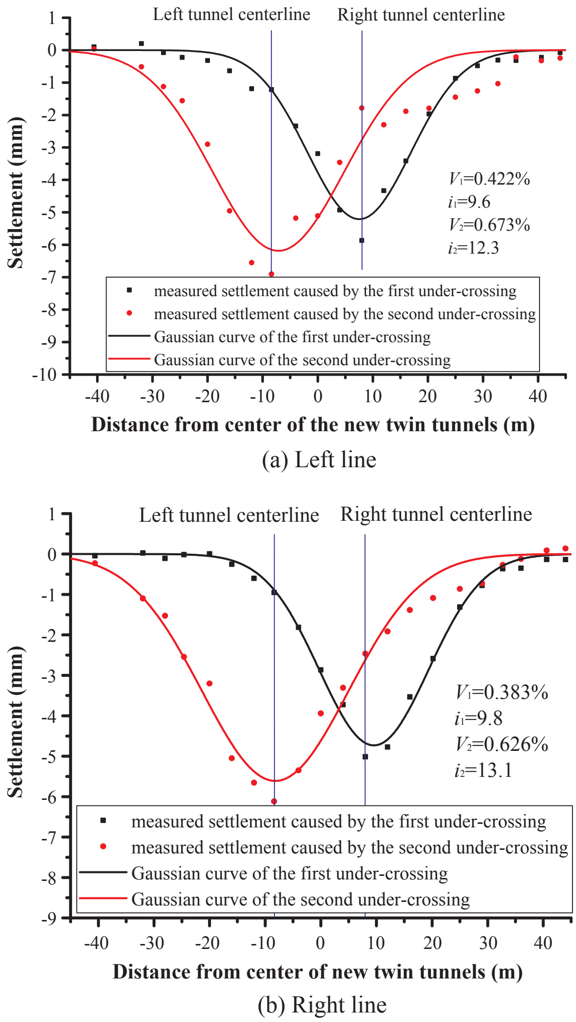

Fig. 15. Fitting settlement profiles caused by each under-crossing alone.

the existing tunnel. In this case, simultaneous back fill grouting with an injection rate of 200% is necessary.

(d) The grouting in the existing tunnel must be handled carefully based on real-time feedback from measured data. The injection volume and pressure of grouting in the existing tunnel play a decisive role in reducing the settlement of existing tunnels. The two-component grout must be injected symmetrically and synchronously to prevent damage to the tunnel lining that can be induced by unevenly distributed loads.

6.2. Twin tunnel interactions and their effects on the overlying tunnel

Ground settlement induced by tunnel excavation has been studied extensively (e.g., Attewell and Yeates, 1984; Mair, 1979; Mair et al., 1993; Peck, 1969; Taylor, 1984). The ground settlement induced by twin tunneling is often equivalent to the superposition of two single tunnels (Divall et al., 2012; Ercelebi et al., 2011; Hunt, 2005; Ocak, 2014; Suwansawat and Einstein, 2007). The Gaussian distribution curve is most widely used to describe the ground settlement caused by tunneling. This method was first proposed by Peck (1969) and was subsequently verified by field and laboratory tests. The equation for describing ground settlement is as follows:

$$S= S_{max}\exp\left(-\frac{x^2}{2i^2}\right) = \frac{AV}{i\sqrt{2\pi}}\exp\left(-\frac{x^2}{2i^2}\right)$$

where x is the distance from the central line of a tunnel, i (or trough width) is the distance from the tunnel center line to the inflection of the trough, S_{max} is the maximum settlement, A is the tunnel cross sectional area, and V is the percentage of ground loss assuming the ground is incompressible; i.e., V = Vs/A, where Vs is the volume loss due to tunneling.

Because a tunnel is a flexible structure, the Peck equation can also be used to describe the settlement profile of an existing tunnel caused by shield tunneling (e.g., Han et al., 2012; Li et al., 2014). However, the construction of twin tunnels in urban environments occasionally affect the adjacent existing tunnel under operation more seriously, and the final settlement is apparently not a simple superposition of two Gaussian distribution curves. The effect of the construction of twin tunnels on the overlying tunnel is also affected by the interactions between the twin tunnels, which are primarily responsible for the asymmetry of the settlement profile. The trough caused by the first shield can be determined using the Peck equation. In addition, to obtain the existing tunnel response induced by the second shield, the additional settlement caused by the second shield passing must be determined. As the settlement of the overlying tunnel remained relatively stable before the second under-passing, the settlement of the existing tunnel induced by the second under-crossing can only be obtained by subtracting the settlement measured after the first shield passing from the settlement measured after the second shield passing. The individual settlement profiles formed by the twin tunnels of Line 9 are shown in Figs. 9 and 10.

A satisfactory match between the fitting curves with the Peck equation and the settlement data of the existing tunnel caused by twice under-crossing was obtained. Obviously, each of the settlement profiles is symmetrical, and the symmetry center is on the tunnel axis. However, a great difference can be observed between the settlement profiles induced by the first shield passing and the second shield passing. The magnitude of the maximum settlement and the size of the zone of influence of the overlying tunnel in the second under-crossings are larger than those of the first under-crossing. The ground loss ratios fit by the Peck equation are 0.422%/0.383% (left line, right line) in the first under-crossing but 0.673%/0.626% (left line, right line) in the second under-crossing, and the width parameters of the settlement trough are 9.6/9.8 in the first under-crossing but 12.3/13.1 in the second under-crossing. Both the ground loss ratio and width parameter of the settlement trough of the second profile are larger than those of the first profile. These differences between the two under-crossings are primarily due to the disturbance of the soil when the first tunnel was built below the existing tunnels and resulting reduction of the stiffness of the soil. These changes are also responsible for the asymmetry of the final settlement profile.

7. Conclusions

This paper presented a case of an in-tunnel grouting protection method for building closely spaced twin tunnels beneath existing tunnels. The protection measures implemented in this project and the related monitoring data were elaborated, and the behavior of the existing tunnels and the characteristics of the influence of shield tunneling on the overlying tunnel were analyzed. The key results obtained from this study can be summarized as follows:

(1) An in-tunnel grouting protection method was adopted to control the deformation of the existing tunnel. This scheme aimed to increase the rigidity of the tunnel lining and compensate for the ground losses caused by the excavation of the new tunnel below. Consequently, the existing tunnel deformation was controlled within the permitted size, and the convergence of existing tunnel deformation was accelerated.

(2) During the design phase, the parameters of grouting control and shield tunneling must be reasonably determined. The use of two-component grouting is suitable to reduce existing tunnel settlement,

and key parameters, including the mix proportions of the grout, the location of the injection holes, and the injection pressure, must be predefined. Important shield tunneling parameters such as the shield advance speed and the rotation of the cutter head should be considered before construction but can be changed during construction development. Real-time feedback from measured data is necessary to adjust the parameters of grouting in the existing tunnel and shield tunneling during construction.

(3) The superimposed effects on the existing tunnel when closely spaced twin tunnels are built below by the shield method can be described in two aspects. (a) First, the final deformation is the superposition of twice under-crossing. After the second under-crossing, the settlement profile is clearly different from the first. The settlement profile changes from a "V" shape to a "W" shape, and the position of maximum settlement is drawn toward the succeeding shield tunnel. (b) Second, the surrounding soil is seriously disturbed when the first tunnel is built beneath the existing tunnel, and the soil stiffness is reduced. When the second tunnel is built, the shield machine is located in the disturbed soil, and large movements of the surrounding soil and the existing tunnel are induced. Consequently, a larger settlement of the existing tunnel occurs, and the interaction of the twin tunnels leads to an asymmetric final accumulated settlement profile after the completion of both tunnels.

(4) The responses of the existing tunnel cross section, including both the additional stress and deformation, reveal three deformation modes based on data obtained from the above project. The change in hoop stress had little influence on the existing tunnel because of the initial stress itself. Compared with the hoop stress, the longitudinal stress of the existing tunnel had a great impact on the structure. The structure carries a load in tension, and the maximum value of the longitudinal stress monitored was approximately 0.63 MPa.

(5) The Peck equation can also be used to describe the settlement profile of an existing tunnel caused by shield tunneling. However, there is a great difference between the settlement profiles induced by the first shield passing and the second shield passing. The magnitude of the maximum settlement and the size of the zone of influence of the overlying tunnel in the second under-crossing are larger than those of the first under-crossing. Both the ground loss ratio and width parameter of the settlement trough of the second profile are larger than those of the first profile. These differences between the two under-crossings mainly resulted from the disturbance of the soil during the construction of the first tunnel below the existing tunnels, which is also responsible for the asymmetry of the final settlement profile.

Acknowledgments

The authors gratefully acknowledge financial support from the National Basic Research Program of China (973 program) under Grant No. 2015CB057800 and the Fundamental Research Funds for the Central Universities under Grant No. 2016YJS109.

References

Attewell, P.B., Woodman, J.P., 1982. Predicting the dynamics of ground settlement and its derivatives caused by tunnelling in soil. Ground Eng. 15.

Attewell, P.B., Yeates, J., 1984. Ground Movements and Their Effects on Structures. Surrey University Press, Guildford, Surrey, UK.

Cooper, M.L., Chapman, D.N., Rogers, C.D.F., Chan, A.H.C., 2002. Movements in the piccadilly line tunnels due to the heathrow express construction. Géotechnique 52, 243–257.

Divall, S., Goodey, R.J., Taylor, R.N., 2012. Ground movements generated by sequential twin-tunnelling in over-consolidated clay. In: Eurofuge 2012, Delft, The Netherlands, April 23–24, 2012. Delft University of Technology and Deltares.

Ercelebi, S.G., Copur, H., Ocak, I., 2011. Surface settlement predictions for Istanbul metro tunnels excavated by EPB-TBM. Environ. Earth Sci. 62, 357–365.

Garshol, K.F., 2003. Pre-excavation grouting in rock tunneling. MBT International Underground Construction Group.

Han, X., Liu, C.W., Standing, J.R., 2012. Structural settlement of existing tunnel caused by new tunnel excavated underneath. China Civ. Eng. J. 45, 134–141 (in Chinese).

Hunt, D.V.L., 2005. Predicting the Ground Movements Above Twin Tunnels Constructed in London Clay, Ph.D. Thesis, University of Birmingham.

Kovári, K., Ramoni, M., 2004. Urban tunneling in soft ground using TBM. In Proceedings of the International Congress on Mechanized Tunneling: Challenging Case Histories, pp. 16–19.

Li, X.G., Yuan, D.J., 2012. Response of a double-decked metro tunnel to shield driving of twin closely under-crossing tunnels. Tunn. Undergr. Space Technol. 28, 18–30.

Li, X.G., Zhang, C.P., Yuan, D.J., 2013. An in-tunnel jacking above tunnel protection methodology for excavating a tunnel under a tunnel in service. Tunn. Undergr. Space Technol. 34, 22–37.

Li, Q., Zhang, D., Fang, Q., Li, D., 2014. Study of deformation characteristics of tunnels traversing adjacently under shield tunnels by shallow tunneling. Chin. J. Rock Mech. Eng. 33, 3911–3918 (in Chinese).

Mair, R.J., 1979. Centrifugal Modelling of Tunnel Construction in Soft Clay, Ph.D. Thesis, Cambridge University.

Mair, R.J., Taylor, R.N., Bracegirdle, A., 1993. Subsurface settlement profiles above tunnels in clays. Géotechnique 43, 315–320.

Ocak, I., 2014. A new approach for estimating the transverse surface settlement curve for twin tunnels in shallow and soft soils. Environ. Earth Sci. 72, 2357–2367.

Oggeri, C., Ova, G., 2004. Quality in tunnelling: ITA-AITES working group 16 final report. Tunn. Undergr. Sp. Tech. 19, 239–272.

Peck, R.B., 1969. Deep excavation and tunneling in soft ground state of the art report. In: 7th International Conference on Soil Mechanics and Foundation Engineering, Mexico City, pp. 225–290.

Fang, Q., Zhang, D., Li, Q., Wong, L.N.Y., 2015. Effects of twin tunnels construction beneath existing shield-driven twin tunnels. Tunn. Undergr. Sp. Tech. 45, 128–137.

Schmidt, B., 1969. Settlements and Ground Movements Associated with Tunneling in Soils. Ph.D. Thesis, University of Illinois at Urbana-Champaign, Illinois.

Suwansawat, S., Einstein, H.H., 2007. Describing settlement troughs over twin tunnels using a superposition technique. J. Geotech. Geoenviron. Eng. 133, 445–468.

Taylor, R.N., 1984. Ground Movements Associated with Tunnels and Trenches. Ph.D. thesis, University of Cambridge.

Kimpritis, T., Smon, W., Pandrea, P., Vukotic, G., 2014. Jet grouting – a solution to problems in tunneling – examples from Europe. 2nd Eastern European Tunnelling Conference.

Wood, A.M., 2002. Tunnelling: Management by Design. CRC Press, Boca Raton.

Yamaguchi, I., Yamazaki, I., Kiritani, Y., 1998. Study of ground–tunnel interactions of four shield tunnels driven in close proximity, in relation to design and construction of parallel shield tunnels. Tunn. Undergr. Sp. Tech. 13, 289–304.

Ye, G.L., Hashimoto, T., Shen, S.L., Zhu, H.H., Bai, T.H., 2015. Lessons learnt from unusual ground settlement during double-o-tube tunnelling in soft ground. Tunn. Undergr. Sp. Tech. 49, 79–91.